Supporting Information for

Sulfamethazine Transformation by Manganese Oxide in Aqueous Solution

Juan Gao[1,2], Curtis Hedman[3,4], Cun Liu[5], Tan Guo[6], and Joel A. Pedersen[,2,3]*

[1]State Key Laboratory of Pollution Control and Resource Reuse, School of the Environment, Nanjing University, Nanjing, PR China, 210093,

[2]Department of Soil Science, University of Wisconsin, Madison, WI, 53706

[3]Wisconsin State Lab of Hygiene, Madison, WI, 53718

[4] Environmental Chemistry and Technology Program, University of Wisconsin, Madison, WI, 53706

[5]Department of Crop and Soil Sciences, Michigan State University, East Lansing, Michigan 48824

[6]Sequoia Foundation/Department of Toxic Substances Control, Berkeley, CA 94710

Text S1. Supporting Information for the Materials and Methods

Chemicals. Sulfamethazine (SMZ), manganese chloride, sodium permanganate, potassium permanganate, sodium acetate, formic acid, and ammonium formate were purchased from Acrōs Organics (Fairland, NJ). A 0.36 mM SMZ stock solution was prepared in 10 mM sodium acetate buffer. [Phenyl-$^{13}C_6$]-SMZ was obtained from Cambridge Isotope Laboratories, Inc. (Andover, MA). *N*-(4,6-dimethylpyrimidin-2-yl) benzene-1,4-diamine was obtained Oakwood Products, Inc. (West Columbia, SC). Hydrochloric acid (12 M), NaCl, and methanol (HPLC grade) were obtained from Fisher Chemicals (Fair Lawn, NJ); glacial acetic acid was acquired from Sigma Chemical Co. (St. Louis, MO); sodium hydroxide was procured from Mallinckrodt Specialty Chemicals Co. (Paris, KY); and oxalic acid was bought from Mallinckrodt Chemical Works (St. Louis, MO). Argon (Ultra high purity, 99.999%) and oxygen (Ultra high purity, 99.995%) were purchased from Linde Gas, LLC. (Independence, OH). Unless otherwise specified, the purities of all chemicals were > 99%.

MnO_2 Synthesis. Manganese oxide was synthesized by the method of Murray.[1] Briefly, 3.2 mmol NaOH was added to 400 mL of 4 mM $NaMnO_4$ under constant stirring, followed by dropwise addition of 24 mL of 0.1 M $MnCl_2$ at room temperature (Mn^{VII}:Mn^{II} = 0.67). After the MnO_2 precipitate formed, the suspension was centrifuged at 6500*g* for 15 min. The precipitate was washed six times with distilled deionized water (ddH_2O; 18 MΩ-cm resistivity; NANOpure Ultrapure Water System, Barnstead, Dubuque, Iowa) to achieve an electrical conductivity < 0.06 $\mu S \cdot cm^{-1}$ at 22.7 °C. The δ-MnO_2 was stored in aqueous suspension at 4 ºC.

MnO_2 Characterization. Scanning electron microscopy (SEM) images were taken using a LEO Supra 1555 VP field emission scanning microscope (Carl Zeiss SMT Ltd, German). Surface area was determined by N_2 adsorption using the Brunauer-Emmett-Teller (BET) method

at room temperature on a Micrometrics ASAP 2010 multi-gas volumetric adsorption analyzer. The ζ-potential and aggregate hydrodynamic diameter of the MnO_2 particles were determined by electrophoretic and dynamic light scattering using a Zetasizer Nano ZS (Malvern Instruments, Southborough, MA). The pH_{zpc} of δ-MnO_2 is < 2.4.[1] X-ray diffractometry was conducted on a Scintag PAD V diffractometer (Cupertino, CA) using CuKα radiation and continuous scanning from 2° to 70° 2θ at $0.05°\cdot sec^{-1}$. The x-ray diffraction pattern of the poorly crystalline manganese oxide synthesized resembled that of δ-MnO_2. The oxidation status of δ-MnO_2 was determined by back titration. Briefly, a predetermined amount of δ-MnO_2 was dissolved in excess 0.2 M sodium oxalate. The remaining oxalate was oxidized by dropwise addition of 0.1 M pre-titrated fresh potassium permanganate. The oxidation state of δ-MnO_2 was calculated from the amount of oxalate oxidized prior to permanganate addition.

The δ-MnO_2 produced using the method employed[1] was reported to have hexagonally symmetrical unit cells with random stacked layers.[2] Scanning electron microscopy indicated that the δ-MnO_2 formed aggregates composed of primary particles with diameters of 30 to 70 nm (Figure S2). Back titration of δ-MnO_2 with sodium oxalate and potassium permanganate[3] indicated the average oxidation state of the Mn was +3.94. If the δ-MnO_2 is assumed to contain no Mn^{II}, 94% of the manganese was present as Mn^{IV}, a result consonant with the findings of Villalobos et al.[2] Figure S2 provides further characteristics of the synthesized δ-MnO_2.

Quenching Methods. When oxalic acid was used to halt the δ-MnO_2-mediated reaction, the quench time was defined as the time needed to dissolve 90% of MnO_2,[4] 7 s in these experiments. Quenching by filtration took 2 s to remove remaining MnO_2. The end of a time interval was defined as the sampling time plus the quench time. Preliminary experiments

indicated no detectable reaction of SMZ with oxalic acid and lack of significant SMZ sorption to syringe filters ($p > 0.05$).

Adsorption of SMZ to δ-MnO_2. The degree of SMZ adsorption to δ-MnO_2 was determined by comparing the difference in SMZ concentrations between samples quenched by filtration and by oxalic acid dissolution. The amount SMZ in sample filtrates corresponded to the (operationally defined) free antimicrobial, while that in samples quenched by oxalic acid addition was the total amount of SMZ (sorbed + free). Results from these experiments are presented in Figure S3.

Influence of Temperature. To examine the influence of temperature on SMZ transformation, reactors were housed in an incubator, and all solutions used were pre-equilibrated to the desired temperature.

HPLC-UV Analyses. In kinetics experiments, sample aliquots were analyzed on a Gilson HPLC (pump model 302, manometric module model 802B, sample injector 231) equipped with EC 4.0 mm × 250 mm Nucleosil C18/5 μm column (Macherey-NAGEL Inc., Germany) and Spectra SYSTEM UV2000 detector (Thermo Separation Products, San Jose, CA) set at λ = 254 and 265 nm. An isocratic mobile phase composed of 31% methanol and 69% aqueous formic acid (0.07%) and ammonium formate (10 mM) was used at a 0.8 $mL \cdot min^{-1}$ flow rate.

For product identification, HPLC-UV with full UV scan (λ = 190-400 nm) was used to monitor the disappearance of SMZ and the evolution of chromophore-bearing transformation products. Quenched samples (10 μL) were injected directly on to a Phenomenex Luna 3u C18 (2) column (150 × 3.0 mm) in a Hewlett Packard Series 1050 HPLC equipped with an Agilent 1100 diode array detector. UV spectra for λ = 190-400 nm were collected every 2 s for each 38-

min chromatographic run. A binary mobile phase at a flow rate 0.3 $mL \cdot min^{-1}$ was used: mobile phase A was 90:10 water/acetonitrile (v/v) with 10 mM ammonium formate and 0.07% formic acid, and mobile phase B consisted of acetonitrile. The mobile phase gradient was as follows: 0-5 min, 100% A; 5-15 min, 90% A; 15-25 min, 70% A; 25-30 min, 55% A; 30-34 min, 100% A; 34-38 min, 100% A. After each sample, a method blank was run to minimize carryover between runs.

HPLC-tandem mass spectrometry. HPLC-MS/MS was used to elucidate the structures of SMZ transformation products. The Agilent 1100 HPLC (consisting of an autosampler, column oven, diode array detector, and a binary gradient pump) was interfaced to an Applied Biosystems/MDS SCIEX API 4000 triple quadrupole mass spectrometer. Mobile and stationary phases were identical to those used for HPLC-UV analysis of transformation products; the elution rate was 0.36 $mL \cdot min^{-1}$. Positive ionization mode TurboIonSpray (TIS) mass spectra (25-1000 *m*/*z*, mass resolution = 0.7 *u* FWHM) were collected with a 1-s scan time. MS acquisition parameters included the following: curtain gas pressure = 20 psi, nebulizer gas pressure = 35 psi, drying gas pressure = 30 psi, declustering potential = 51 V, entrance potential = 10 V, collision cell exit potential = 10 V, source temperature = 400 ºC, and capillary voltage = 5500 V. Product Ion Scan MS/MS experiments were conducted under the same HPLC conditions listed above at collision energies of 25 and 50 eV.

HPLC-time-of-flight-mass spectrometry. HPLC-TOF-MS was used to obtain accurate masses and the most probable elemental composition of selected products. A 5 μL aliquot of the filter-quenched reaction mixture was injected directly onto an Agilent Zorbax 1.8 μM SB-C18 (2.1 × 50 mm) column in an Agilent 1100 series HPLC with capillary-LC pumps. The binary mobile phase (flow rate = 0.20 $mL \cdot min^{-1}$) consisted of 0.1% formic acid in ddH_2O for mobile

phase A and 0.1% formic acid in acetonitrile for mobile phase B. The mobile phase gradient was as follows: 0-30 min, B increasing linearly from 1.0% to 100%; 30-32 min, B decreasing linearly from 100% to 1.0%; and 32-35 min, 1.0% B. Samples were ionized in positive electrospray mode at 4.0 kV. The reference masses 922.009798 (HP-0921, $[C_{18}H_{18}O_6N_3P_3F_{24}+H]^+$) and 121.050873 (purine, $[C_5H_4N_4+H]^+$) (Agilent API-TOF reference mass solution kit) were used as locked mass standards, and mass accuracy was 3 ppm.

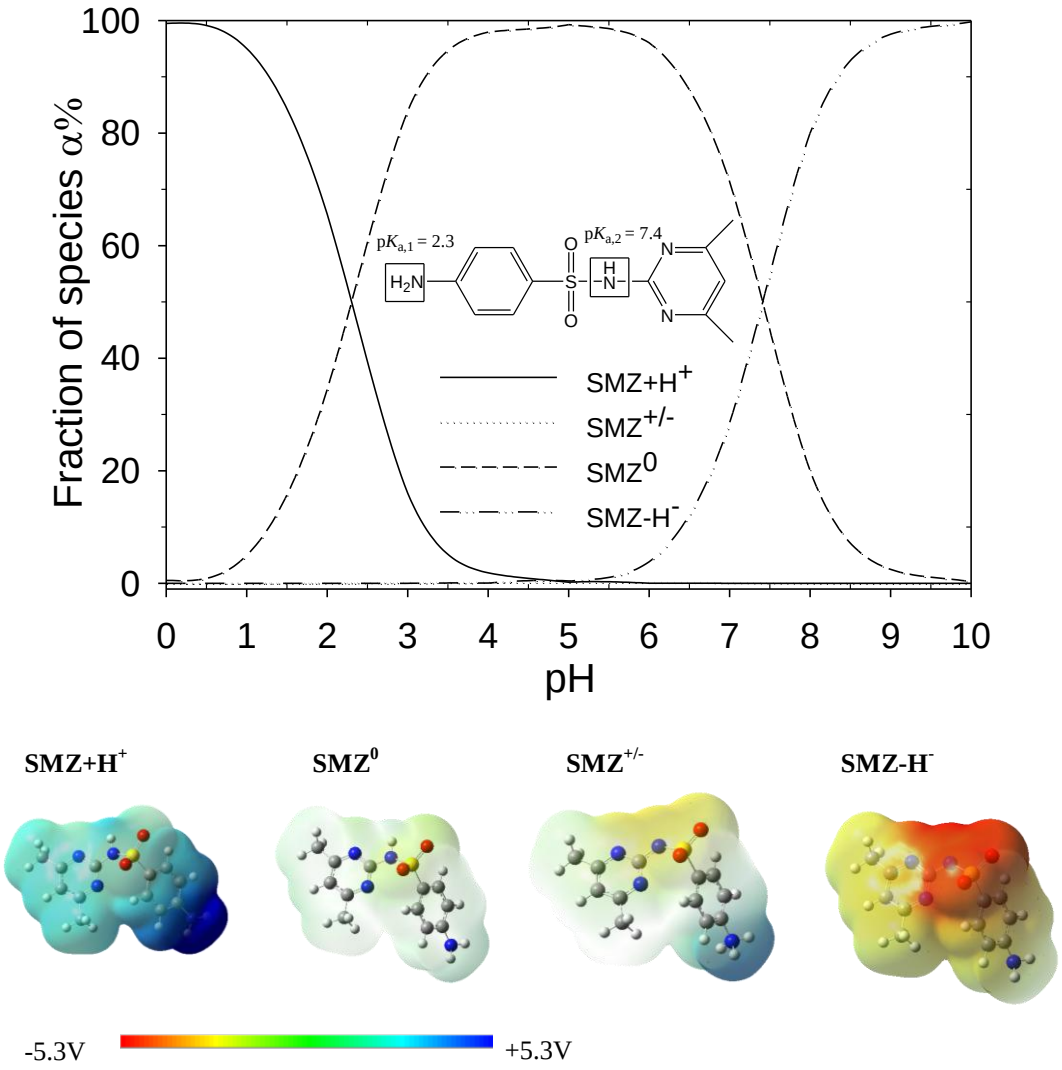

Figure S1. Speciation as a function of pH, skeletal formulae and molecular electrostatic potentials (MEPs) of cationic ($SMZ+H^+$), neutral (SMZ^0), zwitterionic ($SMZ^{\pm}$) and anionic ($SMZ\text{-}H^-$) sulfamethazine species. Macroscopic dissociation constants (pK_a) for SMZ was taken from Lin et al.[5] Molecular electrostatic potentials were calculated along the ρ = 0.0004 e/Å^3 electron density isosurface corresponding approximately to the molecular van der Waals radius. Atoms in the ball-and-stick structures are color-coded as follows: white, H; grey, C; blue, N; red, O; and yellow, S.

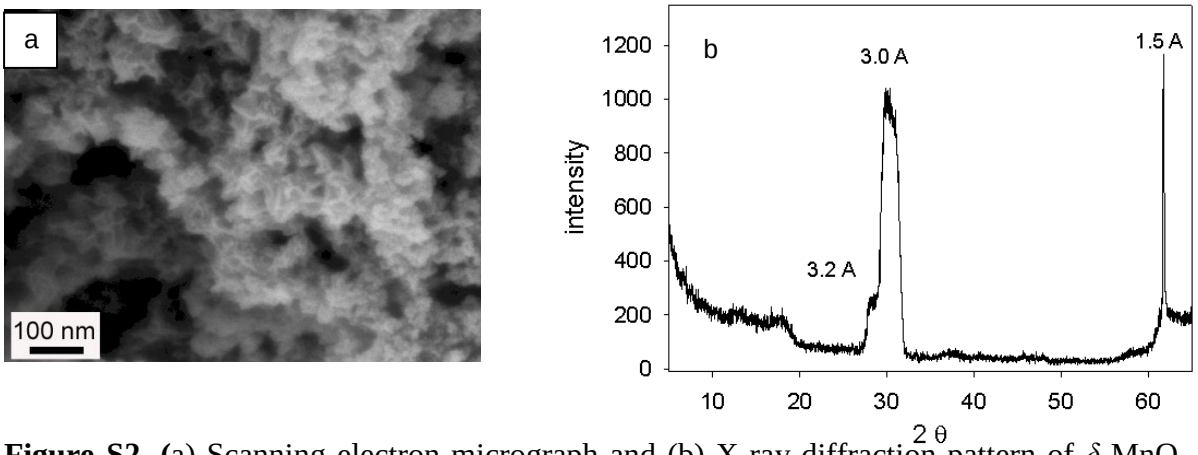

Figure S2. (a) Scanning electron micrograph and (b) X-ray diffraction pattern of δ-MnO_2. For (b), a few drops of aqueous MnO_2 suspension were pipetted onto glass slides and dried at room temperature prior to analysis. The x-ray diffractogram lacked a peak at 7.2 Å, indicating that the *c*-axis of the synthesized δ-MnO_2 was disordered.

Table S1. Properties of the synthesized δ-MnO_2.

parameter	value
hydrodynamic diameter at pH 5.0 (nm)[a]	390 ± 10
A_{surf} ($m^2 \cdot g^{-1}$) [b]	333.28
ζ-potential at pH 5.0 (mV)	-34 ± 5
Mn oxidation state	+3.94
x-ray diffraction peaks (Å)	3.2, 3.0, 1.5

[a] Z-average hydrodynamic diameter determined by dynamic light scattering.
[b] BET surface area determined by N_2 adsorption at room temperature.

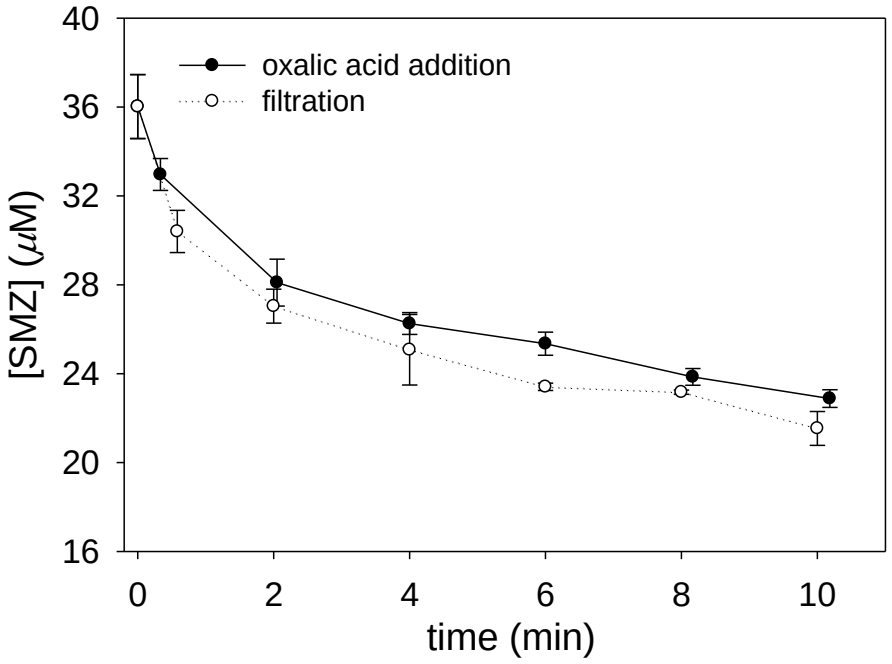

Figure S3. Adsorption of SMZ to δ-MnO_2 at pH 5.0. The amount of SMZ in samples quenched by oxalic acid addition corresponds to the total amount (sorbed + dissolved) of SMZ; the amount of SMZ passing the 0.2-µm filter represents the operationally defined dissolved fraction. Initial concentrations: $[SMZ]_0$ = 36 μM, $[\delta\text{-}MnO_2]_0$ = 360 μM. Reactions were conducted in 10 mM Na acetate with I adjusted to 10 mM by addition of NaCl. Error bars indicate one standard deviation of triplicate measurements.

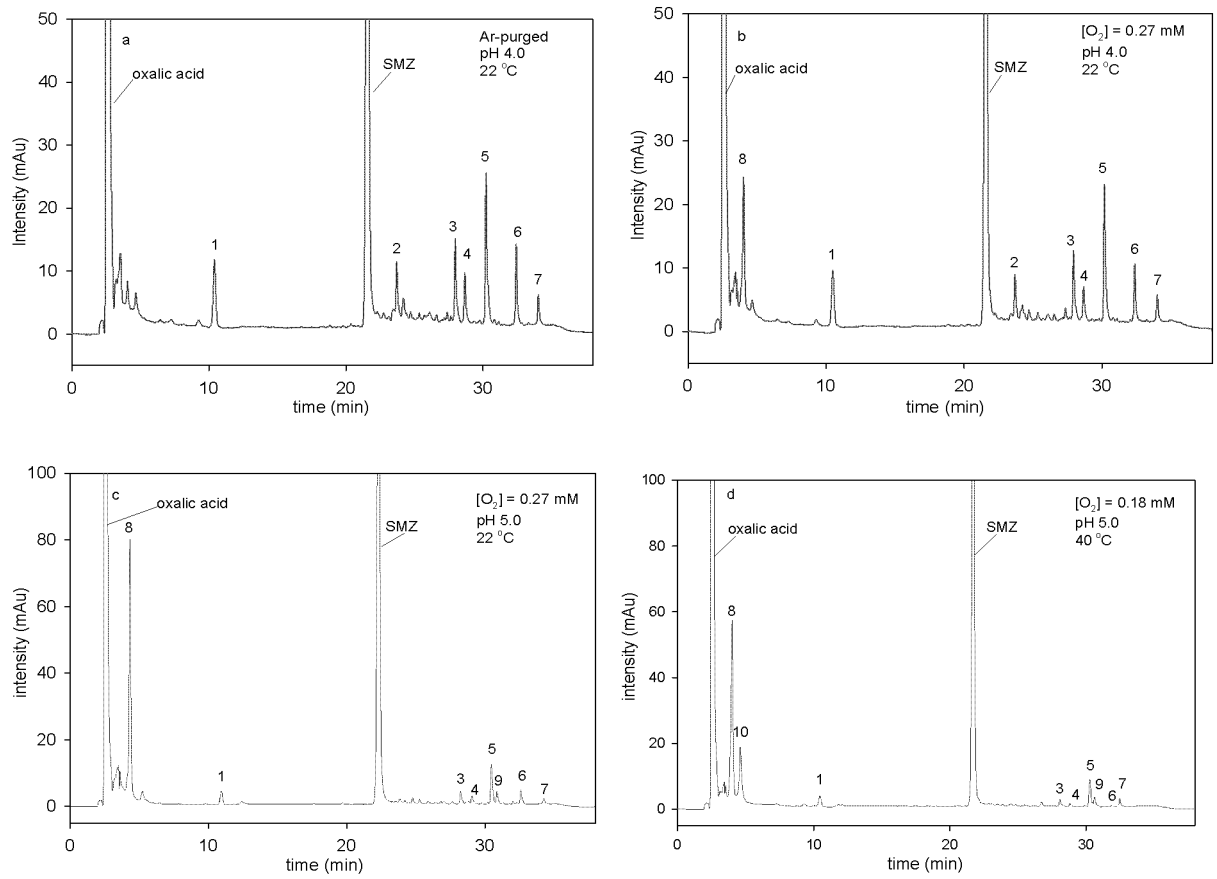

Figure S4. HPLC-UV chromatograms (λ = 254 nm) for δ-MnO_2-mediated transformation of SMZ (t = 10 min) conducted under (a) Ar-purged (O_2-free) conditions at pH 4.0 and 22ºC; (b) ambient O_2 conditions at pH 4.0 and 22ºC; (c) ambient O_2 conditions at pH 5.0 and 22ºC; (d) ambient O_2 conditions at pH 5.0 and 40ºC. For each set of reaction conditions, products profiles were the same at 1 min and 10 min. Comparison of product profiles quenched either by filtration or oxalic acid addition indicated that products **1, 6** and **7** were extensively adsorbed to δ-MnO_2, while **5** and **8** were not (data not shown). At room temperature, **7** and **8** were unstable. During 48-h storage at room temperature in the dark, **8** appeared to partially transform into **10**, **7** was completely degraded (Figure S5), and other product peaks decreased. For all reactions shown, initial concentrations $[SMZ]_0$ = 0.144 mM and $[MnO_2]_0$ = 1.44 mM. Initial dissolved oxygen concentrations for reactions conducted under ambient O_2 conditions: $[O_2]_{aq,\ 22\ °C}$ = 0.27 mM, $[O_2]_{aq,\ 40\ °C}$ = 0.18 mM.

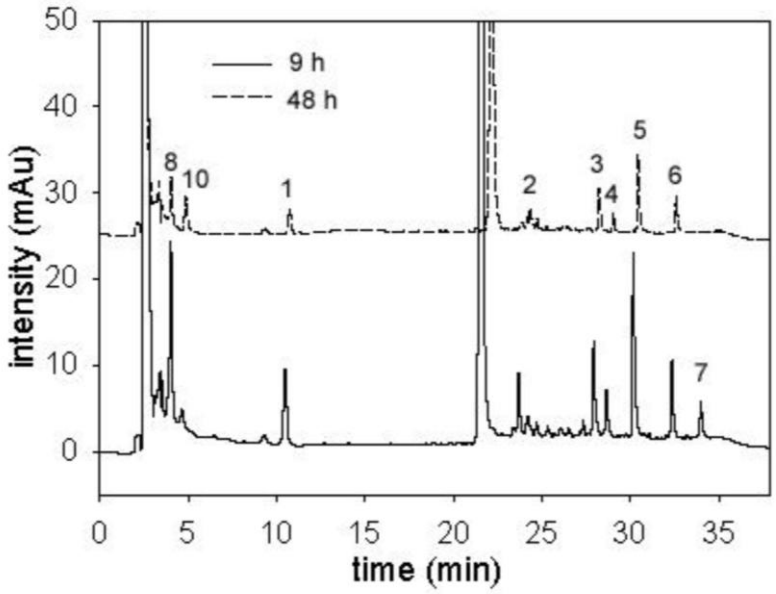

Figure S5. Stability of SMZ transformation products over 48 h. δ-MnO_2-mediated transformation of SMZ was conducted at pH 4, $[O_2]_{aq}$ = 0.27 mM, and 22 ºC. Reactions were quenched at t = 10 min with oxalic acid and stored at room temperature for 9 and 48 h in dark. HPLC-UV profiles were constructed for λ = 254 nm.

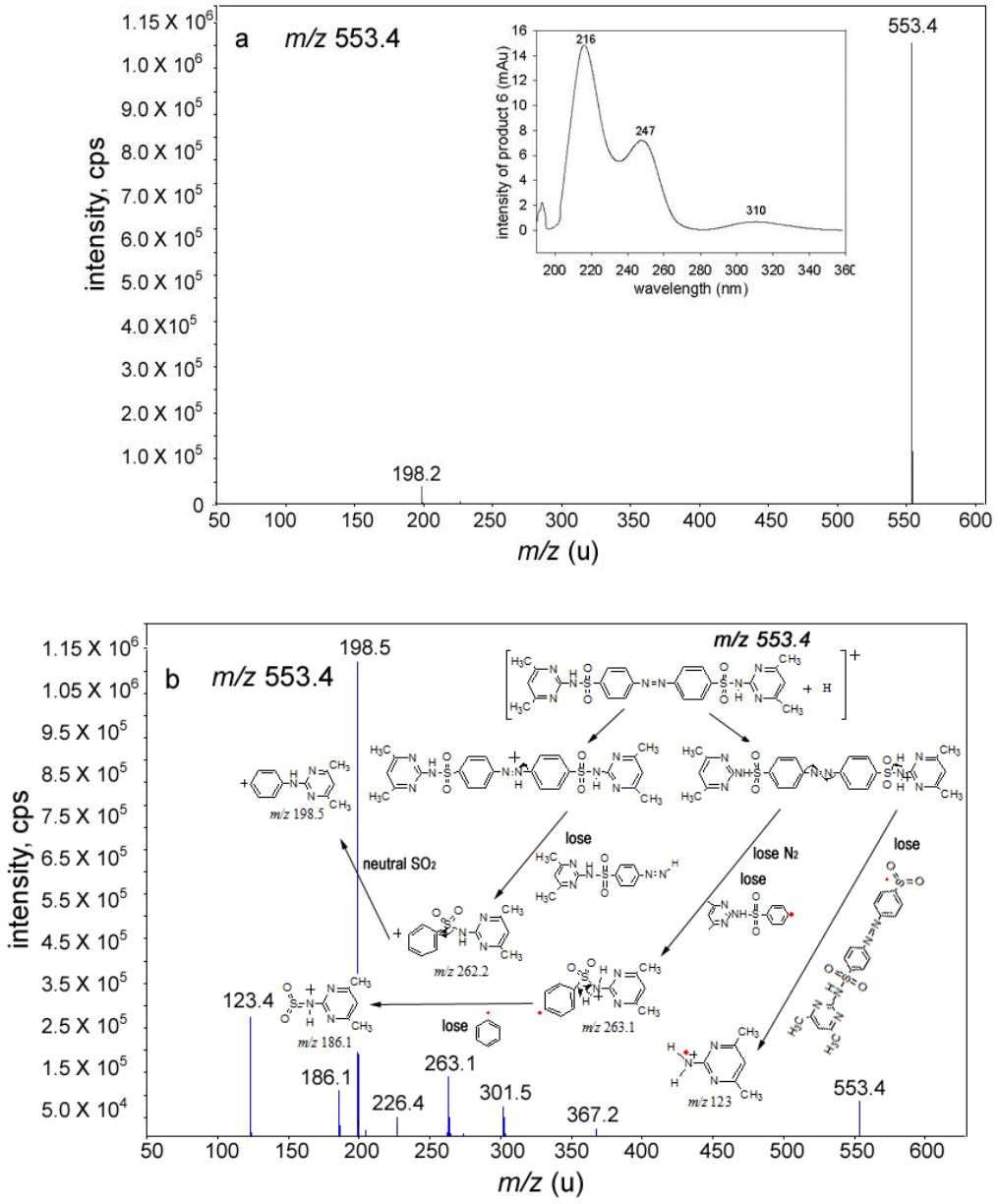

Figure S6. MS^2 spectra of **5** (*m/z* 553.4) obtained by CAD at (a) 25 eV and (b) 50 eV. The inset in (a) shows the UV spectrum for **5** in 10 mM ammonium formate; the inset in (b) shows proposed detailed fragmentation pathways for **5** with a 50 eV collision energy. Multiple protonization sites (azo-N and sulfonal-amide-N) were possible for **5**.

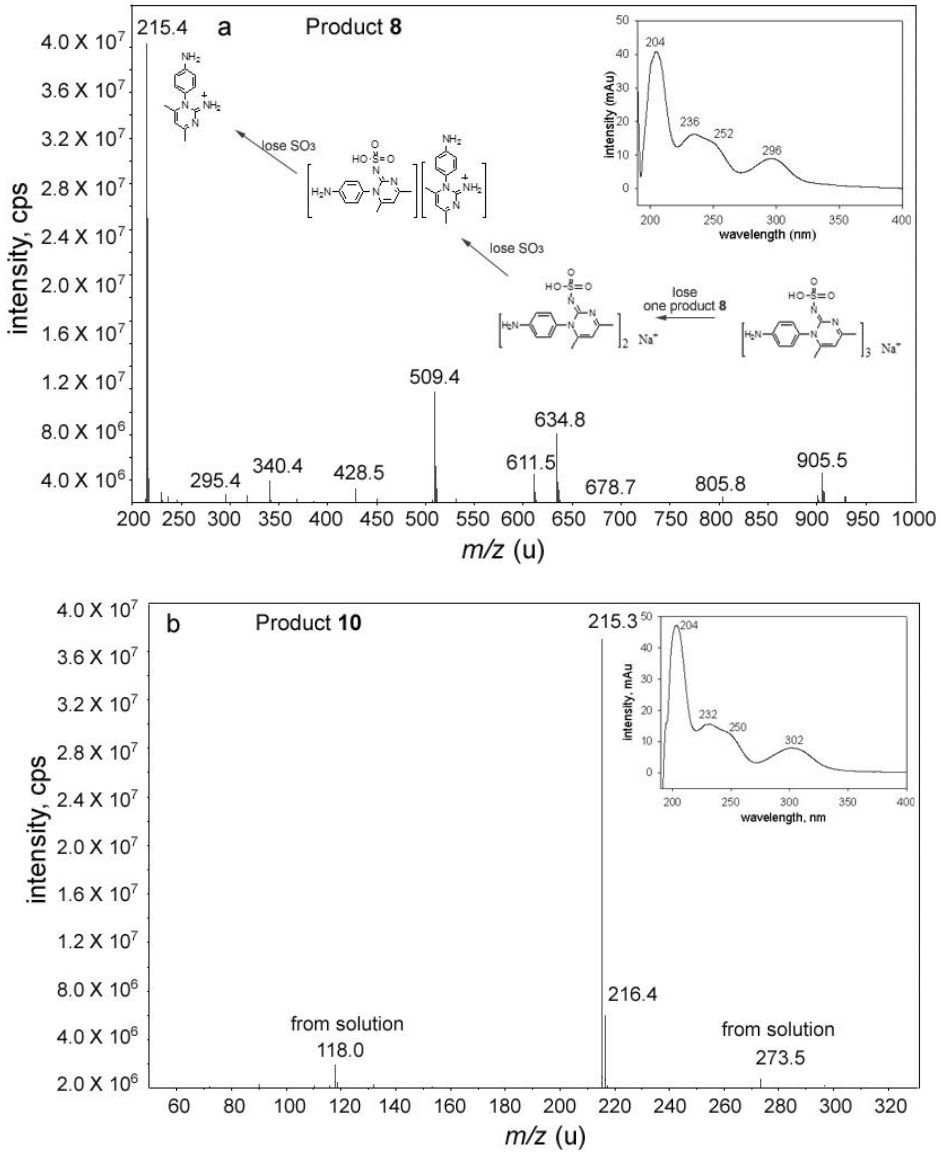

Figure S7. Full-scan mass spectra of (a) Product **8** and (b) Product **10**. The insets contain the corresponding UV spectra (with maximum absorbance wavelengths noted).

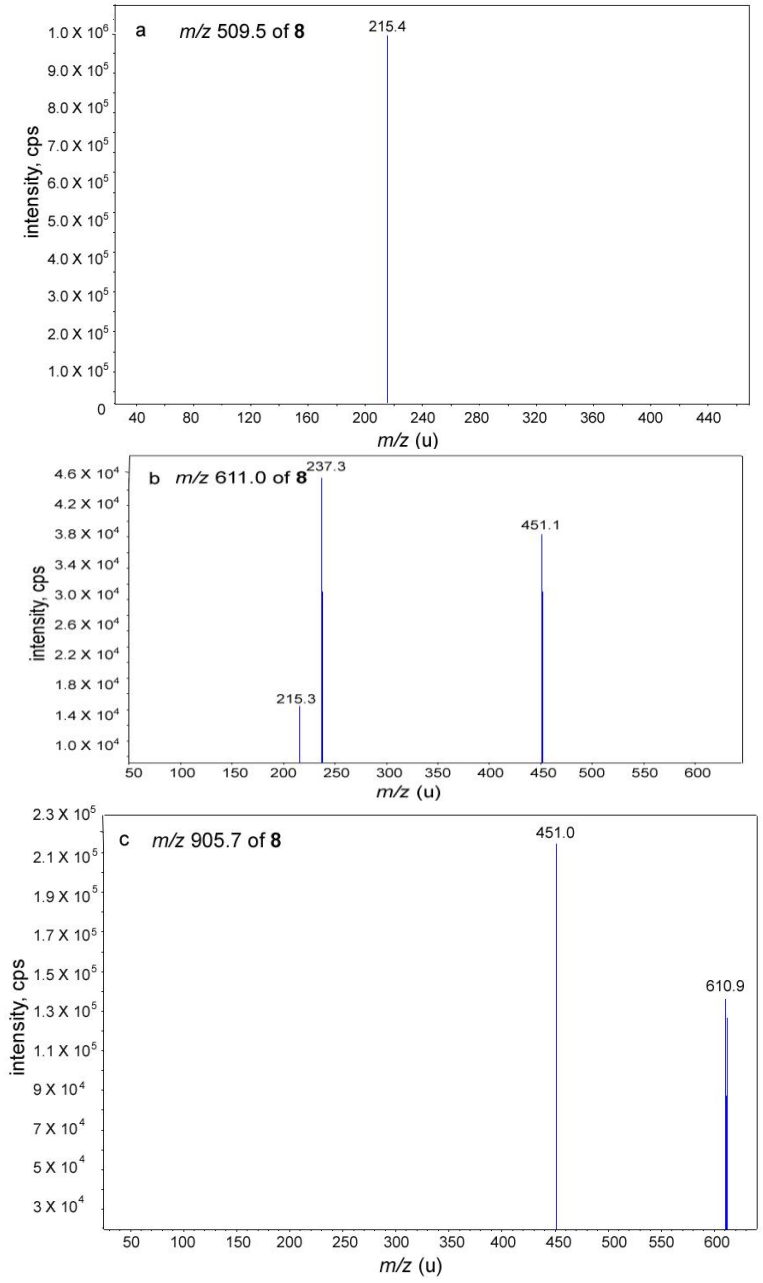

Figure S8. MS^2 spectra of selected ion clusters in the full-scan mass spectrum of **8** (*cf*. Figure S7a): (a) *m*/*z* 509.5, (b) *m*/*z* 611.0 and (c) *m*/*z* 905.7. CAD was conducted at 25 eV.

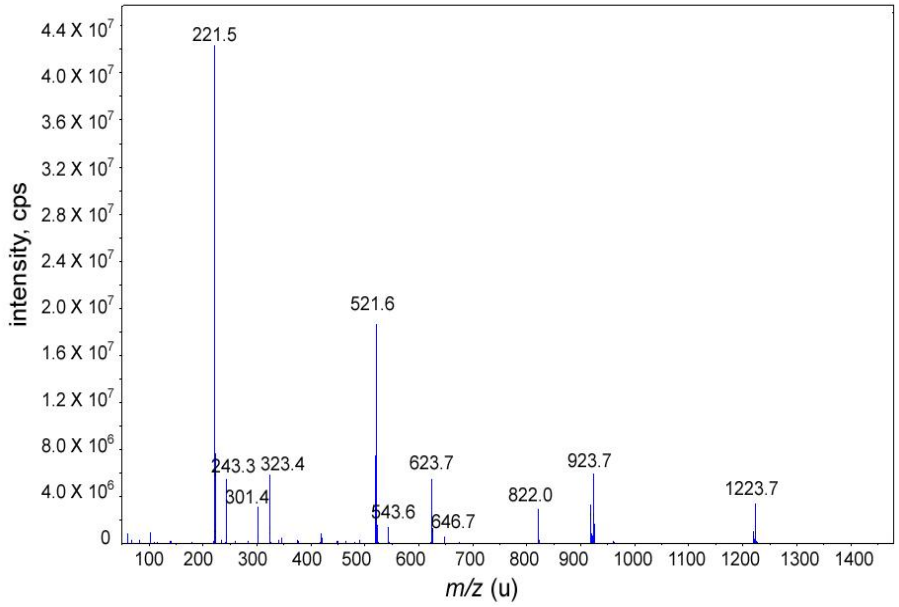

Figure S9. Full-scan mass spectra of phenyl-$^{13}C_6$ labeled **8**. MS^2 spectra of the *m/z* 221.5 daughter ion are shown in Figure S10.

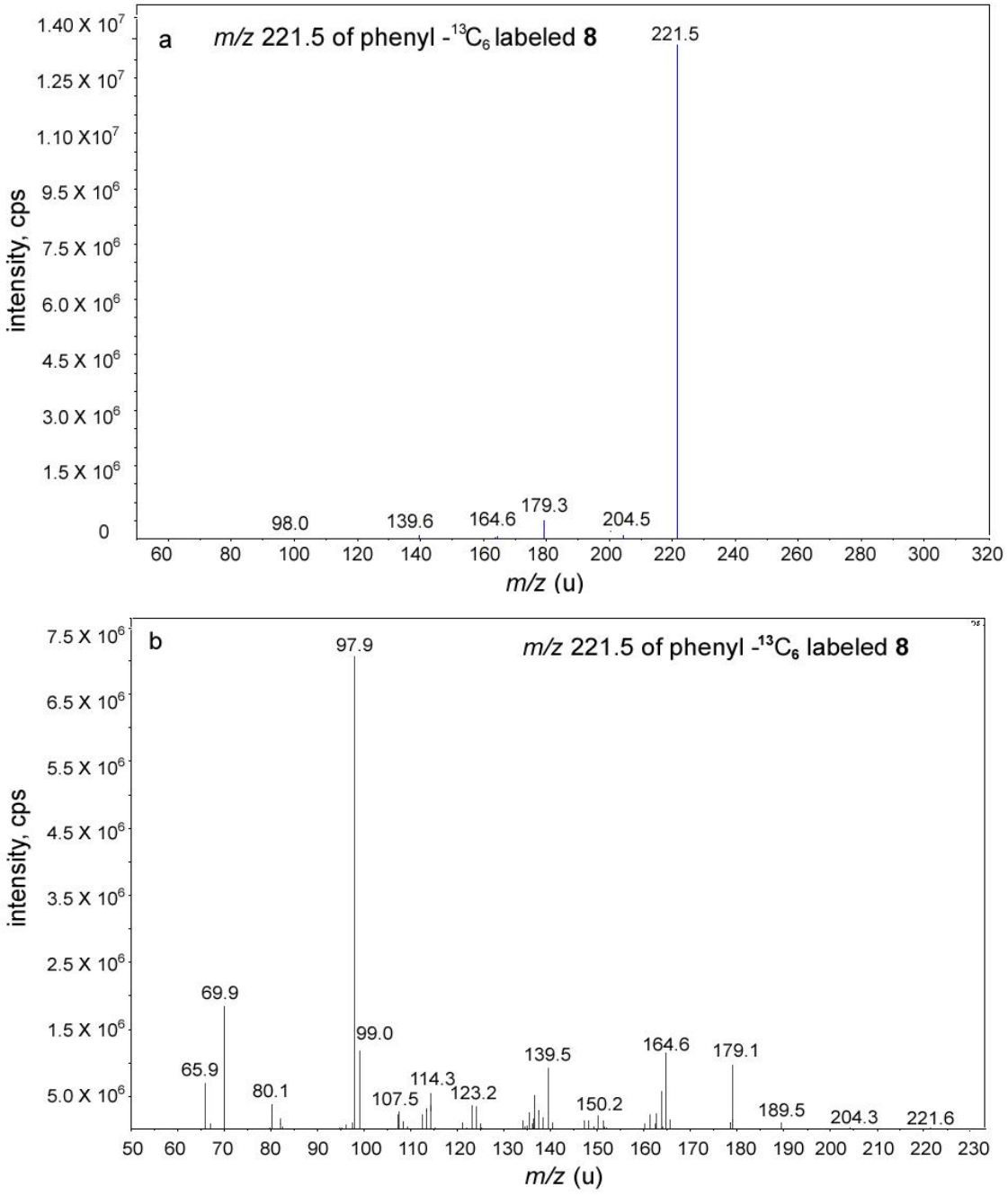

Figure S10. MS^2 spectra of the *m*/*z* 221.5 daughter ion phenyl-$^{13}C_6$-labeled **8** obtained with CAD conducted at (a) 25 eV and (b) 50 eV. The fragment ions with *m*/*z* = 139.6, 164.6, 179.3 and 204.5 were 6 *u* heavier than those with *m*/*z* 133.2, 158.3, 173.3 and 198.7 appearing in the MS^2 spectra of daughter ion *m*/*z* = 215.4 of **8** (*cf*. Figure 2b).

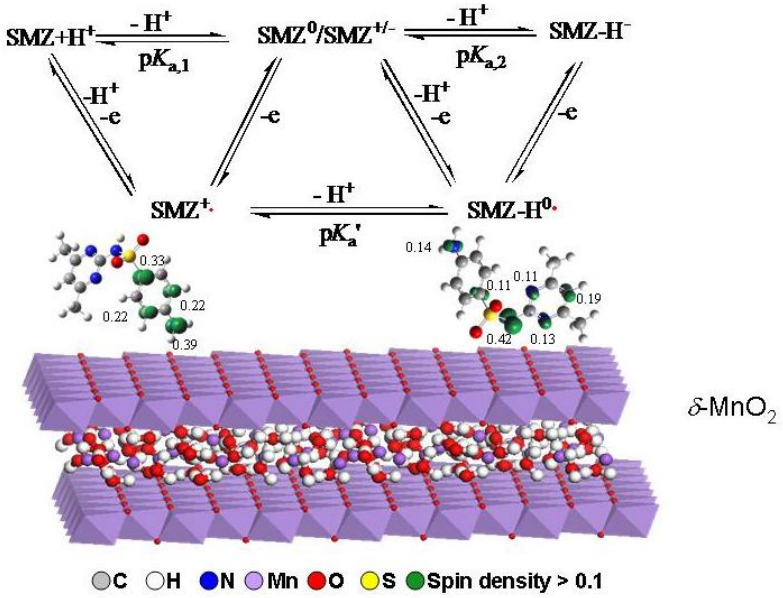

Scheme S1. Speciation of SMZ and SMZ radicals. The p$K_{a,1}$ and p$K_{a,2}$ were from Lin et al.[5] The macroscopic proton dissociation constant for the radical species of pK_a' = 5.2 has been reported.[6] The DFT/PCM optimized radical structures are shown in ball and stick representation with spin density isosurface at 0.0675 e Å^{-3} plotted. Numbers are atomic spin densities calculated by NBO analysis.

Text S2. Relative energy among SMZ radical resonance structures.

One electron (e^-) could be transferred from SMZ aniline N (N4) group or sulfonal amide (N1) group to Mn^{III}/Mn^{IV} on δ-MnO_2 surface to form an SMZ radical species (Scheme S1). The equilibrium between cationic and neutral radical species is pH dependent, and the fraction of the cationic radical ($SMZ^{+}\cdot$), $\alpha_{SMZ+\cdot}$, can be expressed as:

$$\alpha_{SMZ^{+}\cdot} = \frac{1}{1+10^{pH-pK'_a}} \qquad S1$$

Due to rotation about the S−N1 bond, two stable conformational isomers of SMZ or SMZ radicals are possible: an anti rotamer (dimethylpyrimidine and 2 O on different sides of S-N1 bond) and a syn rotamer (dimethylpyrimidine and 2 O on the same side of S-N1 bond). Solvated DFT/PCM calculations indicated that the relative free energies of formation were lowest for the anti rotamers of the N4 radicals for both $SMZ^{+}\cdot$ and $SMZ\text{-}H^{0}\cdot$ (Figure S13; $SMZ^{+}\cdot$ (N4) syn could not be located). $SMZ^{+}\cdot$ (N4) anti was therefore predicted to be the dominant radical cationic species (Figure S13a). For the neutral radical, the relative free energy differences among the $SMZ\text{-}H^{0}\cdot$ (N1) anti, $SMZ\text{-}H^{0}\cdot$ (N1) syn, $SMZ\text{-}H^{0}\cdot$ (N4) anti and $SMZ\text{-}H^{0}\cdot$ (N4) syn species were less than 11.0 $kJ\cdot mol^{-1}$, and co-existence of all four radicals were expected.

Table S2. Evaluation of possible structures for Product 8.

Label	Structure	Name	$\Delta_r G^{\dagger}$ (kJ·mol^{-1})
SMZ-N1-OH	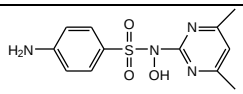	4-amino-*N*-(4,6-dimethylpyrimidin-2-yl)-*N*-hydroxybenzenesulfonamide	+47.3
SMZ-N→O	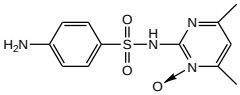	sulfamethazine-*N*-oxide	+20.6
SMZ-*p*-OH	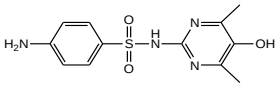	4-amino-*N*-(5-hydroxy-4,6-dimethylpyrimidin-2-yl)benzenesulfonamide	−117.7
SMZ-Smiles	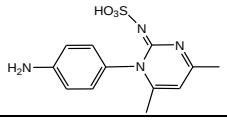	1-(4-aminophenyl)-4,6-dimethylpyrimidin-2(1*H*)-ylidenesulfamic acid	−120.4 (SMZ-Smiles-SO_3 conformer 1) −149.5 (SMZ-Smiles-SO_3 conformer 2)

† Free energies of reaction ($\Delta_r G$) of the evaluated structure relative to the reference state, SMZ+½O_2, computed using B3LYP/6-31+G* with the PCM solvent model. See main text for further details.

$MnO_2 + 4H^+ + 2e^- \rightarrow Mn^{2+} + 2H_2O$ ($E_H^0 = 1.29$V)[7] has the similar standard reduction potential as ½$O_2 + 2H^+ + 2e \rightarrow H_2O$ ($E_H^0 = 1.23$V),[8] so O_2 was used to simplify the calculation. PCM, polarizable continuum model.

Table S3. Free energies of reaction ($\Delta_r G$) for formation of Product 5 computed using B3LYP/6-31+G* with the PCM solvent model.

Proposed reaction pathway	$\Delta_r G^{\dagger}$ (kJ·mol^{-1})
Hydrazo route	
2 SMZ-H^{0}· (N4) → azoHH-SMZ	−183.6
azoHH-SMZ + $^{1}/_{2}$ O_2 → azo-SMZ + $H_2O^{\ddagger}$	−127.9
Nitrene route	
2 SMZ-H^{0}· (N4) + $^{1}/_{2}$ O_2 → 2[SMZ-nitrene triplet rad]^{0}·· + H_2O	−11.8
2[SMZ-nitrene triplet rad]^{0}·· → azo-SMZ	−299.7

† Free energies of reaction ($\Delta_r G$) for the proposed pathways computed using B3LYP/6-31+G* with the PCM solvent model. See main text for further details.
$^{\ddagger}MnO_2 + 4H^+ + 2e^- \rightarrow Mn^{2+} + 2H_2O$ ($E_H^0 = 1.29$V)[7] has the similar standard reduction potential as $^{1}/_{2}$ $O_2 + 2H^+ + 2e^- \rightarrow H_2O$ ($E_H^0 = 1.23$V)[8], so in this calculation O_2 is used to simplify the calculation.

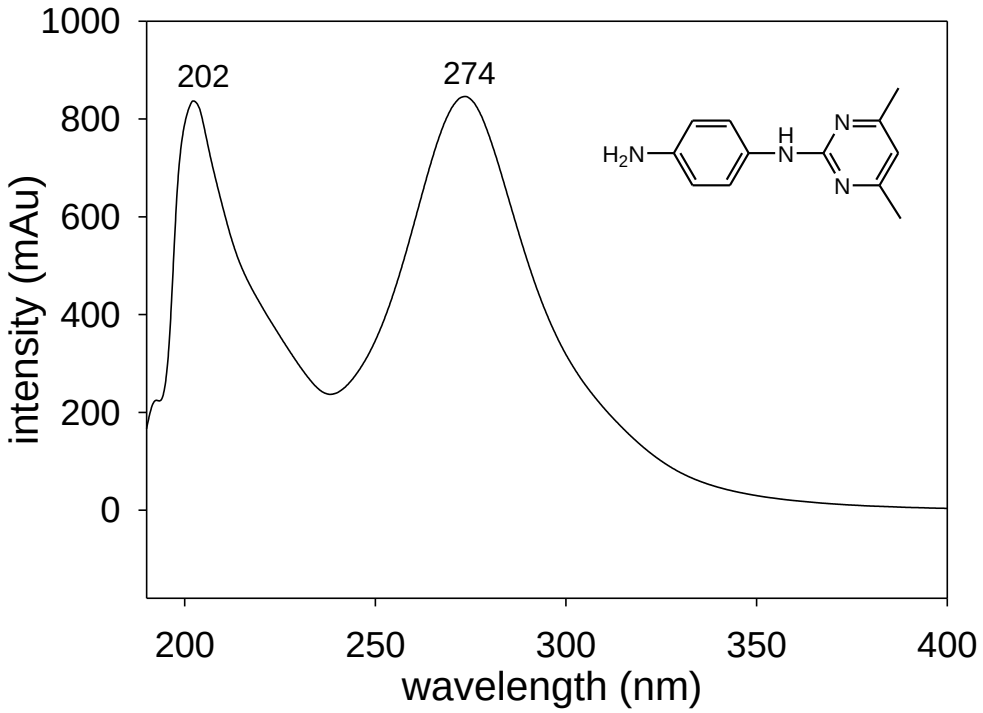

Figure S11. UV spectrum of *N*-(4,6-dimethylpyrimidin-2-yl)benzene-1,4-diamine.

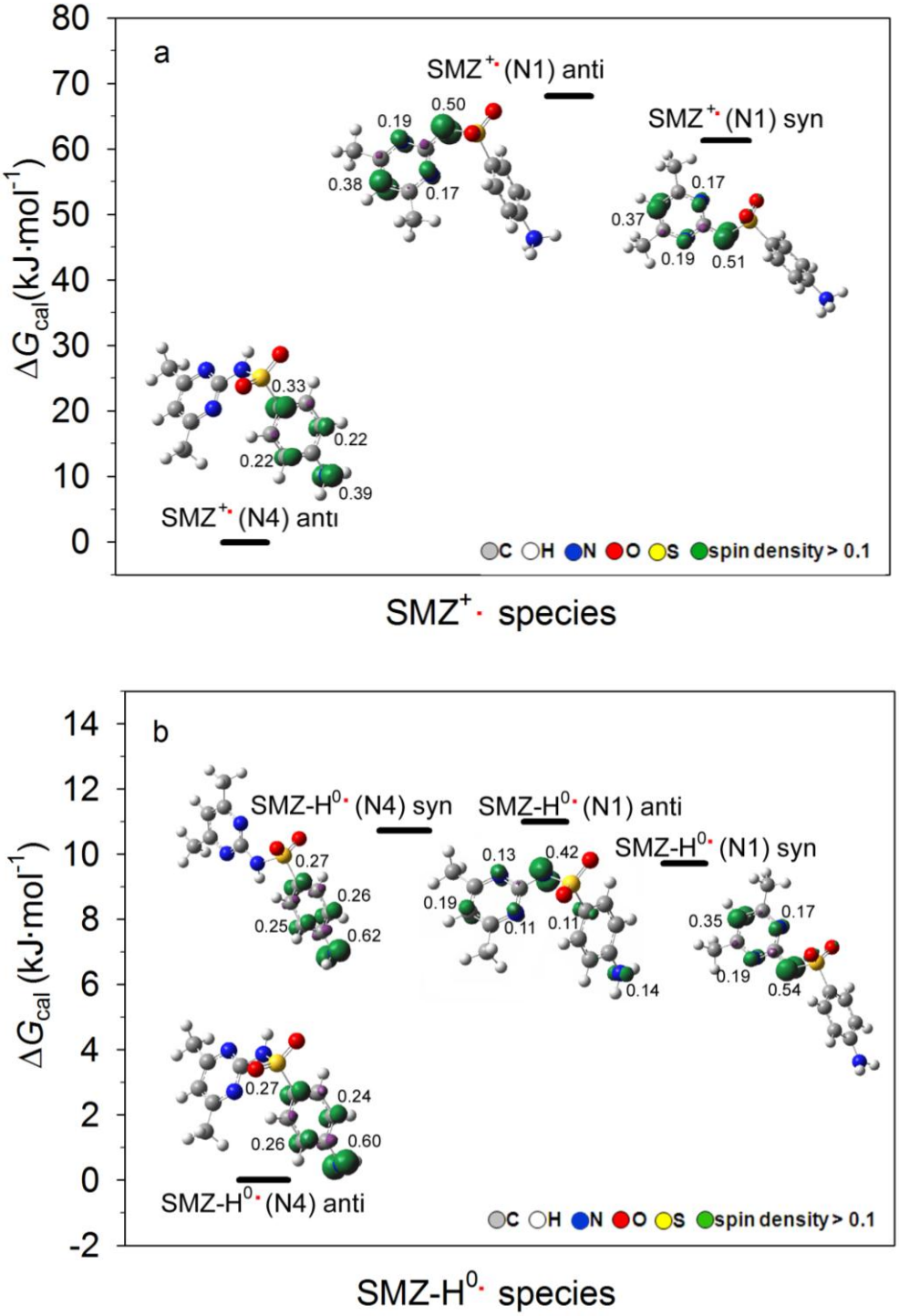

Figure S12. Relative free energies of formation in aqueous phase (calculated by PCM/DFT method) for (a) cationic radical ($SMZ^{+}\cdot$) and (b) neutral radical ($SMZ^{0}\cdot$) species. The structures represent ball-stick stereoisomers of $SMZ^{+}\cdot$ and $SMZ^{0}\cdot$ radical species with spin density isosurface at 0.0675 e $Å^{-3}$ plotted. Numbers are atomic spin densities calculated by NBO analysis.

Text S3. Literature Cited

1. Murray, J. W., Surface chemistry of hydrous manganese-dioxide. *J. Colloid Int. Sci.* **1974,** *46*, 357-371.
2. Villalobos, M.; Toner, B.; Bargar, J.; Sposito, G., Characterization of the manganese oxide produced by *Pseudomonas putida* strain Mnb1. *Geochim. Cosmochim. Acta* **2003,** *67*, 2649-2662.
3. Skoog, D. A.; West, D. M.; Holler, F. J., *Fundamentals of Analytical Chemistry*. Saunders College Publishing USA: TX, 1992.
4. Rubert, K. F.; Pedersen, J. A., Kinetics of oxytetracycline reaction with a hydrous manganese oxide. *Environ. Sci. Technol.* **2006,** *40*, 7216-7221.
5. Lin, C. E.; Chang, C. C.; Lin, W. C. Migration behavior and separation of sulfonamides in capillary zone electrophoresis. 2. Positively charged species at low pH. *J. Chromatogr. A* **1997**, *759*, 203-209.
6. Voorhies, J.D.; Adams, R.N. Voltammetry at solid electrodes. Anodic polarography of sulfa drugs. *Anal. Chem.* **1958**, *30*, 346-350.
7. Bricker, O.P. Some stability relations in the system MnO_2-H_2O at 25°C and one atmosphere total pressure. *Am. Mineral.* **1965**, *50*, 1296-1354.
8. McBride, M.B. 1994. *Environmental Chemistry of Soil*. Oxford University Press, New York.